Author(s): Jelovica, Jasmin & Romanoff, Jani

Title: Global buckling and post-buckling of web-core sandwich and stiffened panels: sensitivity to general corrosion

Year: 2014

Version: Final published version

Please cite the original version:

Jelovica, Jasmin & Romanoff, Jani. 2014. Global buckling and post-buckling of web-core sandwich and stiffened panels: sensitivity to general corrosion. Proceedings of the 7th International Conference on Thin-Walled Structures (ICTWS 2014).

Proceedings of the ICTWS 2014 7th International Conference on Thin-Walled Structures
ICTWS2014
28 September – 2 October 2014, Busan, Korea

ICTWS2014-xxxxxx

GLOBAL BUCKLING AND POST-BUCKLING OF WEB-CORE SANDWICH AND STIFFENED PANELS: SENSITIVITY TO GENERAL CORROSION

Jasmin Jelovica, Jani Romanoff
Department of Applied Mechanics, Aalto University
Espoo, Finland

ABSTRACT

Corrosion can lead to reduction of structural stiffness and strength. This paper investigates the influence of a reduction in the thickness of the plates as a result of general corrosion on sandwich panel buckling load and onset of plasticity. The results are compared to the stiffened panel of the same in-plane and bending stiffness. Current guidelines for corrosion protection threat these two structures equally. Load-shortening curves are obtained with the finite element method, with the kinematics being represented using two approaches: (1) equivalent single-layer with first-order shear deformation theory, and (2) a three-dimensional model of the actual geometry of the structure, modeled using shell and connector elements. The former is also used to identify the influence of corrosion on the stiffness coefficients and, consequently, the buckling load, also via analytical equation. The decrease of the buckling load is found higher in sandwich panel than in stiffened panel. The reduction is especially high in the case of the diffusion of moisture (water) into the core. The reason for the higher sensitivity of sandwich panel is a larger reduction of transverse shear stiffness opposite to the stiffener direction due to corrosion.

1. INTRODUCTION

Sandwich panels are known to have lower weight for the same load-carrying capacity as traditional structures, i.e. stiffened panels and isotropic plates. This makes them interesting to industry and can potentially reduce the carbon footprint which is nowadays a legislation requirement. Selection of steel as a material for sandwich panels makes them easy to incorporate into large assemblies such as bridges, ships, and offshore structures, while still offering weight reductions in comparison to traditional structure. Exposure to humid environment, however, leads to the risk of corrosion and associated reduction of structural stiffness and strength. This can cause unexpected structural failures and thus endanger human lives and environment.

One of the promising types of steel sandwich panels is a web-core panel which consists of unidirectional web plates in the core, welded to the face plates by laser welding. Currently, the guidelines on protection from corrosion threat stiffened panel and web-core sandwich panel the same (Det Norske Veritas, 2004). However, recent studies have shown that the sandwich panel is sensitive to plate thinning because of corrosion. Jelovica *et al.* (2013) performed a series of bending tests on beam specimens previously submerged into the sea for up to two years. The geometry of the cross-section which was tested is standard in industry. Ultimate load was reduced by 10% in one-year corroded and by 17% in two-year corroded beams. The study was extended to plates under in-plane compression in Jelovica *et al.* (2014). The study was conducted by means of numerical and analytical methods, basing the corrosion scenario on geometrical and material changes in the cross-section observed in earlier experimental study. The reduction of buckling load and the load at onset of plasticity were found significant. Here we extend the study by making comparison to stiffened panel. Our aim is to compare the buckling load reduction rates between the two structures which are suspected not to be the same since the topology of the cross-section is different. The motivation comes from the fact that the guidelines against corrosion presently threat them equally.

The plates are studied here under compressive in-plane force since this is one of the main types of loading for the plates in a deck of a ship or bridge girder. The behavior of stiffened

panel in compression has been extensively studied; see e.g. Paik and Thayamballi (2003), Guedes Soares and Gordo (1997), Gordo and Guedes Soares (2011). Byklum and Amdahl (2002) and Byklum *et al.* (2004) have developed a two stage approach for the buckling and post-buckling assessment of stiffened panels. Local buckling is calculated first and the non-linear *ABD*-matrix is derived for global analysis. However, the investigations do not consider the influence of out-of-plane shear deformations. These have shown to have high influence on the response of web-core sandwich panel; see Romanoff and Varsta (2007), Nordstrand (2004) and Jelovica *et al.* (2012).

In difference to stiffened panel, web-core sandwich panel under in-plane compression has only been investigated in a few studies. Kolsters (2004) studied the local buckling and post-buckling behavior of face plates. Taczala and Banasiak (2004) presented the difference in buckling mode and critical stress between sandwich and stiffened panel. Kozak (2006) studied the ultimate strength of sandwich columns. Jelovica *et al.* (2012) studied the influence of laser-weld stiffness on global buckling load of sandwich panels. Laser-weld stiffness is ratio of the moment to the rotation angle at the face-plate-web-plate intersection. Jelovica and Romanoff (2013a) studied geometrically non-linear load-carrying behavior of web-core sandwich panels. The plate response was compared to isotropic plate of the same bending stiffness. Jelovica and Romanoff (2013b) compared the load-carrying behavior of sandwich panel, stiffened panel and isotropic plate. The reasons for differences in their response were outlined in terms of *ABD* and D_Q stiffness coefficients.

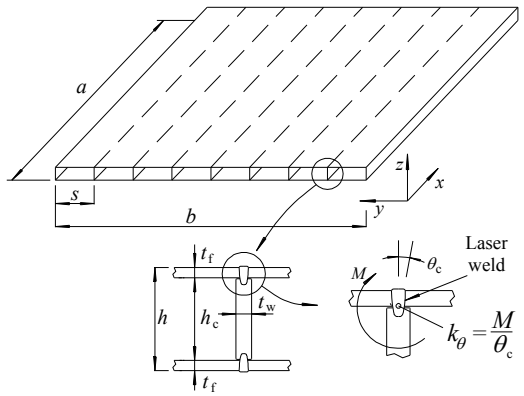

Figure 1. A laser-welded web-core sandwich panel.

We carry out this study using finite element method (FEM) to trace the non-linear load-shortening path, obtain the buckling loads and determine the onset of yielding. Three-dimensional shell element models of the plates are created for this purpose. Furthermore, buckling load is validated with analytical equation where the plates are represented with their *ABD* and D_Q stiffness coefficients. This allows us to relate the differences in the plate behavior to their topology. We study lightweight, slender plates which typically buckle globally. Simply supported boundary condition is considered with loaded edges kept straight and unloaded edges free to move in-plane. Linear-elastic material behavior is used.

2. CORROSION SCENARIO

Several types of corrosion exist, including general corrosion, pitting, grooving, crevice, etc. The most prevalent form of corrosion is a general loss of surface material; this condition results in a gradual thinning of the structure. In this study, general corrosion is considered, since the results from Jelovica *et al.*, (2013) and Det Norske Veritas (2003) indicate that the sandwich panel is affected by this type of corrosion in the most severe conditions, for a limited amount of time. It was furthermore found that corrosion had negligible effect on the welds from those same specimens; see Aromaa *et al.* (2012).

On the basis of these experimental observations, we assume that corrosion causes a uniform reduction in the thickness of the plates and has a negligible effect on the laser weld, i.e. pitting or crevice corrosion does not occur. Thickness reduction occurs in two ways: (1) outside the sandwich panel structure (Figure 2a) and (2) both outside and inside the sandwich panel structure simultaneously (Figure 2b). In the former case, the corrosion reduces the thickness of the face plate t_f on the outer side by the amount $t_{c,out}$, while the thickness of the web plate t_w and height of the core h_c remain the same. In the latter case, the corrosion reduces the thickness of the face plate by $t_{c,in\&out}$ on both sides, causing a reduction in the thickness of the face plate that is twice as high as in the previous case. The thickness of the web plate is also reduced by $t_{c,in\&out}$ on both sides. The corrosion in the core increases the height h_c by $2t_{c,in\&out}$. The weld is considered intact.

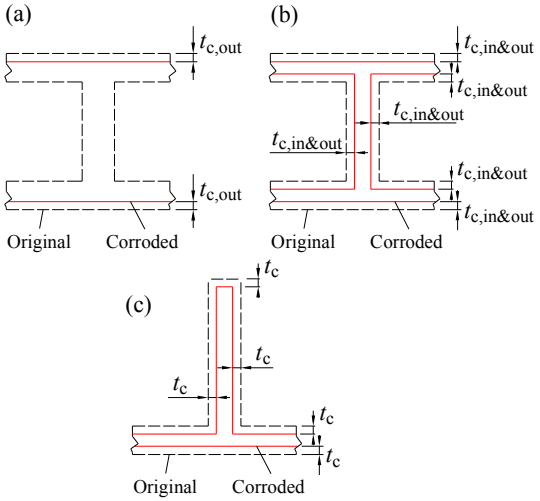

Figure 2. Considered cases of corrosion in a) sandwich panel from outside; b) sandwich panel from inside and outside the structure; c) stiffened panel.

Thickness reduction of stiffened panel is presented in Figure 2c. Thickness is decreased equally in all surfaces. Many studies have shown thickness reduction rates as a function of

time. However, these were found to oscillate quite much, e.g. in ships, where numerous micro-climate conditions are encountered in different spaces of the structure. To avoid the issue of non-linear progress of corrosion with time, this study relates the corrosion solely to the thickness reduction. This can be related to time if necessary, knowing the actual environmental conditions near the plate surface. For example, the literature shows that the average of 0.1 mm/year per exposed surface can be expected for immersed plates in the water flow (Melchers *et al.* 2010). The same was observed in Jelovica *et al.* (2013).

3. ANALYSIS METHODS

Buckling and geometric non-linear analysis are carried out with FEM using the two aforementioned approaches, namely the equivalent single-layer (ESL) theory approach and the three-dimensional (3D) model of the structure. The ESL results are directly affected by the reduction in the plate stiffness coefficients, while the 3D model gives more accurate deformations and stresses because it uses the actual geometry of the corroded structure. In addition, global buckling load of the sandwich and stiffened panel is calculated with available analytical equation for orthotropic plate.

Geometric non-linear analysis is carried out by increasing the compressive load on the imperfect structure in small steps. Shape and magnitude of different production and exploitation imperfections has been measured for stiffened panels in numerous studies (see ISSC 2009 for summary on imperfections) and their influence on behavior in compression presented (Paik 2007, Masaoka and Mansour 2008). However, such studies have not been shown for web-core sandwich panel. Thus in the current study the first eigenmode is used as the shape of the initial imperfection to be consistent between the two structures.

Imperfection is given the magnitude of 0.01% of the plate length. The analysis is carried out using the finite element software Abaqus, version 6.11-2, with the modified Riks algorithm to trace the post-buckling path. A subspace iteration solver is used for the eigenvalue analysis.

Analytical equation for buckling load

Both sandwich and stiffened panel are represented through in-plane ([***A***]), bending ([***D***]), coupling ([***B***]) and transverse shear ([$\boldsymbol{D}_{\mathbf{Q}}$]) stiffness coefficients. Analytical equation for global buckling load of the uni-axially loaded plate following FSDT is (Reddy, 2000):

$$N_0 = \frac{1}{\alpha^2}\left(s_{33} - \frac{s_{34}S_{55} - s_{35}S_{45}}{S_{44}S_{55} - S_{45}S_{45}} s_{34} - \frac{s_{35}S_{44} - s_{34}S_{45}}{S_{44}S_{55} - S_{45}S_{45}} s_{35} \right) \qquad (1)$$

where

$$\alpha = m \cdot \pi / a$$

$$\beta = n \cdot \pi / b$$

$$s_{11} = A_{11} \cdot \alpha^2 + A_{33} \cdot \beta^2$$

$$s_{12} = (A_{11} + A_{33}) \cdot \alpha \cdot \beta$$

$$s_{14} = B_{11} \cdot \alpha^2 + B_{33} \cdot \beta^2$$

$$s_{15} = (B_{12} + B_{33}) \cdot \alpha \cdot \beta$$

$$s_{22} = A_{33} \cdot \alpha^2 + A_{22} \cdot \beta^2$$

$$s_{25} = B_{33} \cdot \alpha^2 + B_{22} \cdot \beta^2$$

$$s_{33} = D_{Qx} \cdot \alpha^2 + D_{Qy} \cdot \beta^2$$

$$s_{34} = D_{Qx} \cdot \alpha$$

$$s_{35} = D_{Qy} \cdot \beta$$

$$s_{44} = D_{11} \cdot \alpha^2 + D_{33} \cdot \beta^2 + D_{Qx}$$

$$s_{45} = (D_{12} + D_{33}) \cdot \alpha \cdot \beta$$

$$s_{55} = D_{33} \cdot \alpha^2 + D_{22} \cdot \beta^2 + D_{Qy}$$

$$b_0 = s_{11} \cdot s_{22} - s_{12} \cdot s_{12}$$

$$b_1 = s_{14} \cdot s_{22} - s_{12} \cdot s_{15}$$

$$b_2 = s_{11} \cdot s_{15} - s_{12} \cdot s_{14}$$

$$b_3 = s_{15} \cdot s_{22} - s_{12} \cdot s_{25}$$

$$b_4 = s_{11} \cdot s_{25} - s_{12} \cdot s_{15}$$

$$S_{44} = s_{44} - s_{14}\frac{b_1}{b_0} - s_{15}\frac{b_2}{b_0}$$

$$S_{45} = s_{45} - s_{15}\frac{b_1}{b_0} - s_{25}\frac{b_2}{b_0}$$

$$S_{55} = s_{55} - s_{15}\frac{b_3}{b_0} - s_{25}\frac{b_4}{b_0}.$$

Here a and b are the length (x-direction) and the width (y-direction) of the plate, respectively. m and n are the number of buckling half-waves in x- and y-direction, respectively, both taken as 1 in this study since they give the lowest buckling load and FEM analyses confirmed it to be the critical shape.

Corrosion changes the cross-section of the plates and therefore the stiffness coefficients, in turn altering the buckling load.

2D models

The buckling and geometric non-linear analysis is carried out using the FEM program Abaqus, version 6.11-2. Equivalent stiffness properties are assigned to a single layer in the geometrical mid-plane of the structure, where the loads and boundary conditions are also defined. Shell elements with four nodes (S4) are used. The mesh consists of 100 elements in the length direction and 100 elements in the width direction. Sensitivity of results to mesh size is presented in Appendix C. The transverse deflection is zero at the edges and no rotation is

allowed about the axis perpendicular to the edge on the loaded sides; that is, the edges are required to stay straight.

3D models

The 3D geometry of the sandwich panel is modeled using shell elements (S4). Connector-type elements (CONN3D2) are used to connect the web and face plate at their intersection. The moment-angle relationship for the connector elements is defined from experimental results (Romanoff *et al*. 2007) to represent the rotational stiffness of the T-joint. Concentrated nodal forces act at the nodes in the neutral axis. Six shell elements per web plate height are used. The face plates have six shell elements between the webs.

Simply supported boundary conditions are considered, with the loaded edges kept straight and the unloaded edges free to move in-plane. The transverse deflection is zero only at the nodes at the geometric mid-plane. This allows the rotation of the plate around the mid-plane edge. Furthermore, all the nodes of a certain web plate have the same displacement v in the y-direction; see Figure 3. Additionally, the nodes at the geometric mid-plane at $x = 0$ are required to have the same displacement u in the x-direction. The same is required at $x = a$.

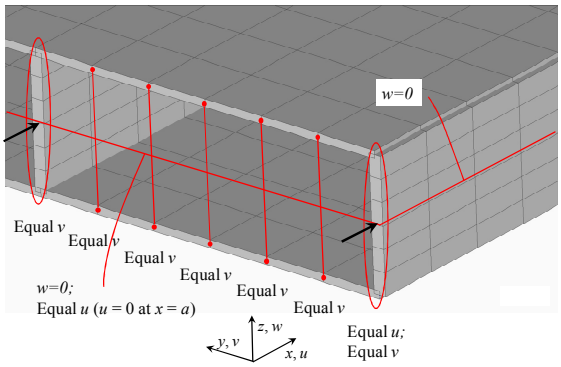

Figure 3. FE mesh and boundary conditions for the 3D model of the sandwich panel.

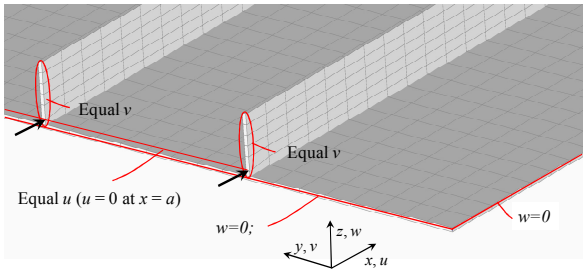

Figure 4. FE mesh and boundary conditions for the 3D model of the stiffened panel.

Stiffened panel is modeled with shell elements (S4). Concentrated nodal forces act on the nodes in the neutral axis. Eight elements between the stiffeners are used. The height of the stiffener is divided in six elements. Influence of mesh density on the results is presented in Appendix C. Deflection constraint is imposed on the plate edges and stiffeners are not able to rotate; see Figure 4. Further, plate edges at x=0 and x=a are required to stay straight.

4. CASE STUDY

The sandwich panel that is studied is a standard web-core sandwich panel for marine and civil applications. The thickness of the face plates is 2.5 mm and the web plate 4 mm. Height of the core is 40 mm and spacing of the web plates is 120 mm. The area weight of the sandwich panel is 50 kg/m^2. The rotational stiffness of the T-joint is taken as 107 kNm/m (Romanoff *et al.* 2007). Dimensions of the stiffened panel are selected such that the structure has the same in-plane and bending stiffness in loading direction as the sandwich panel; see Table 1. The same in-plane stiffness also means that the plates have the same area weight. Thickness of the plate and the stiffeners is 5 mm. Height of the stiffeners is 80 mm and they are 0.3 m apart. The type of the stiffener is a flat bar.

Table 1. Stiffnesses of the considered sandwich and stiffened panel.

	Sandwich panel t_f / t_w × h_c / s	Stiffened panel t_p / FB / s [mm]
	2.5 / 4 x 40 / 120	5 / 80 x 5 / 300
β_{local}	$48\cdot\sqrt{\sigma_y/E}$	$60\cdot\sqrt{\sigma_y/E}$
A_{11} [MN/m]	*1 406*	*1 406*
A_{22} [MN/m]	1 132	1 132
A_{12} [MN/m]	339	339
A_{33} [MN/m]	396	396
D_{11} [kNm]	*548*	*548*
D_{22} [kNm]	511	80
D_{12} [kNm]	153	24
D_{33} [kNm]	179	28
B_{11} [kN]	0	0
B_{22} [kN]	0	9 394
B_{12} [kN]	0	2 818
B_{33} [kN]	0	3 287
D_{Qx} [kNm]	$68\cdot10^3$	$273\cdot10^3$
D_{Qy} [kNm]	*419*	*330* $\cdot10^3$

The calculation of in-plane, bending, coupling and shear stiffness coefficients is presented in Appendix A for the sandwich panel and in Appendix B for the stiffened panel. The values are tabulated in Table 1. It can be seen that sandwich panel has much lower shear stiffness than the stiffened panel, especially in the transverse direction. Sandwich panel is symmetrical with respect to its neutral axes and thus the coupling coefficients are zero, while that is not the case with stiffened panel. Further, breadth to thickness ratio, b/t, (representing the local plate slenderness β) is somewhat lower in sandwich panel.

Jelovica *et al.* (2013) measured corrosion rates for the same sandwich panel as studied here for an exposure time of a

maximum of two years. In their work both cases of outer corrosion only or both inner and outer corrosion were observed. The thickness reduction rate was, on average, 0.1 mm/year per exposed surface. This was found to be in line with the measurements by Melchers *et al.* (2010) for immersed plates.
For analysis using ESL, the stiffness coefficients are calculated on the basis of analytical expressions (Appendix A and B). For 3D analysis, the thickness is modified directly.

The size of the panels is 3.6 m × 3.6 m. The material behavior is assumed to be linear elastic, characterized by a Young's modulus E = 206 GPa and a Poisson's ratio ν = 0.3.

Influence of general corrosion on stiffness coefficients

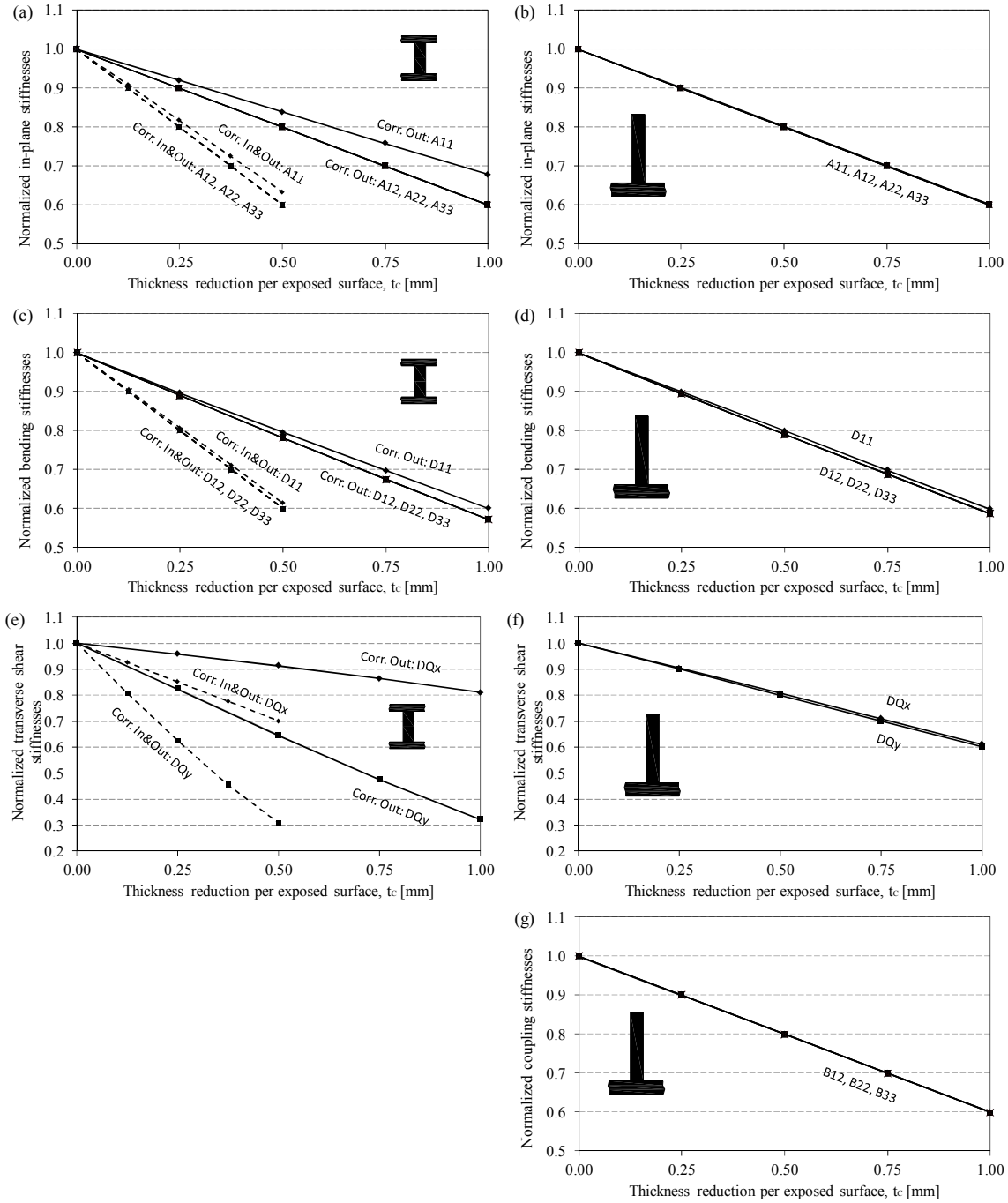

Figure 5. Influence of corrosion on plate stiffness: (a),(b) in-plane; (c),(d) bending; (e),(f) transverse shear and (g) coupling.

Figure 5 shows the reduction of stiffnesses for the sandwich and stiffened panel because of general corrosion. The stiffnesses are calculated with respect to the neutral axis in stiffener direction, for each corrosion case separately. Stiffnesses are normalized by dividing them with their corresponding value for uncorroded panel. Two series of curves are presented for sandwich panel, corresponding to the two corrosion scenarios. It can be seen that the reduction of the stiffnesses is linear in both structures, except for some small non-linearity in transverse shear stiffness for sandwich panel at larger thickness reductions. The decrease in in-plane and bending stiffness is almost the same between the two types of structures, i.e. at 1.0 mm thickness reduction, the in-plane and the bending stiffnesses are at 60% of starting values. Coupling stiffnesses for stiffened panel decrease at the same rate, except for B_{11} which is always zero. The difference between the stiffened and the sandwich panel is in transverse shear stiffness: in stiffened panel, D_{Q} decreases at the same rate as the other stiffnesses, while in sandwich panel the reduction in D_{Qy} occurs at two times higher rate. At 1.0 mm thickness reduction, D_{Qy} for sandwich panel is at 30% of the starting value.

Furthermore, it can be seen that the corrosion of the core causes a rate of reduction of stiffness that is twice as high as only corrosion outside the sandwich panel. In this case, both surfaces of the face plate are exposed to corrosion and thus the total reduction of the thickness is double that of the single side.

Influence of general corrosion on buckling load

Figure 6 presents the decrease in the buckling load resulting from the reduction of the thickness in the two structures. The real values are presented in (a) and the normalized values are presented in (b). The sandwich panel in uncorroded condition has two times higher buckling load than the stiffened panel; however, the rate of reduction is higher in sandwich panel (see Figure 6b). This is especially seen in the case where all surfaces decrease thickness in the sandwich panel. For a decrease in the thickness of 0.5 mm, the reduction of the buckling load is 20% in the stiffened panel, 25.5% in the sandwich panel with outer corrosion and 51% in the sandwich panel with inner and outer corrosion. Reduction of buckling load is linear in both structures, following the linear reduction of stiffness coefficients.

The reason for the different buckling load reduction between the two structures lies in stiffness coefficients. Jelovica and Romanoff (2013b) showed that the buckling load of a stiffened panel is significantly reduced due to asymmetry of the structure (B-matrix different than zero). If the coupling stiffnesses of stiffened panel in this study are put to zero (being the same as for sandwich panel), the buckling load increases to 2.16 MN (+ 40%), however, the rate of buckling load reduction remains the same, i.e. the curve is exactly the same as the one in Figure 6b. Empty B-matrix means that A-matrix has no effect on the buckling load of the stiffened panel. Reduction of the bending stiffness is the same between the two structures, therefore D-matrix is not the cause of different buckling load reduction. The value of the transverse shear stiffness is for stiffened panel practically infinite, i.e. it has no effect on the buckling load. However, transverse shear stiffness D_{Qy} of a sandwich panel is much lower, at a range where it has very strong influence on the buckling load (see Jelovica *et al.* 2012). Among all stiffnesses, corrosion has the highest influence on D_{Qy} (see Figure 5e). Therefore, the reason for higher buckling load reduction in sandwich panel in comparison to stiffened panel is the reduction of D_{Qy}.

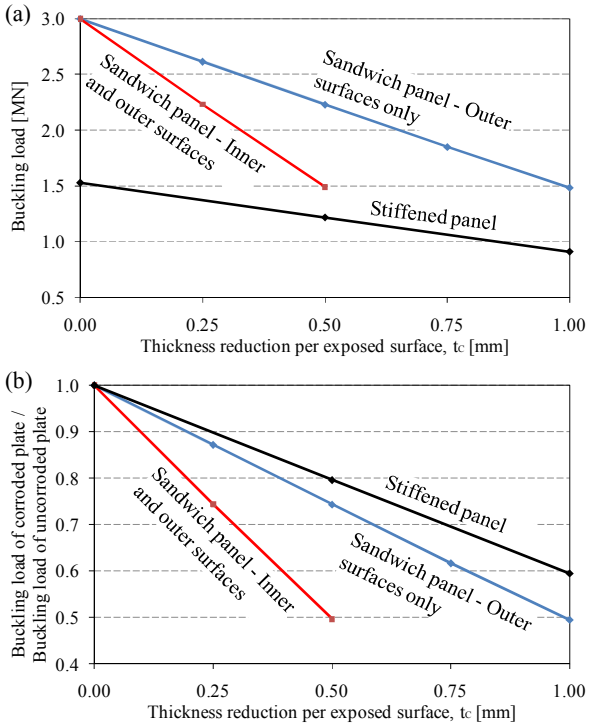

Figure 6. Influence of general corrosion on the: (a) actual buckling load; (b) normalized buckling load.

Influence of general corrosion on non-linear behavior

The load-shortening curves of the sandwich panel with the corrosion of the outer surfaces are presented in Figure 7(a). The load-shortening curves of the stiffened panel are presented in Figure 7(b). The results with both the 2D and 3D models are presented, showing excellent agreement between the two. Therefore, the stiffness coefficients are accurate.

The buckling load agrees closely with the analytical values, being about 1% higher for the 3D solution. The 3D solution is presented until the onset of plasticity, defined here as the point where the von Mises stress at any point in the panel reaches 355 MPa. Beside the reduction of the buckling load, the corrosion also reduces the pre- and post-buckling stiffness of the plate. The load at which the yielding occurs in sandwich panel is reduced in the same rate as the buckling load, i.e. 25% for 0.5 mm thickness reduction and 49% for 1.0 mm thickness reduction. Corrosion of all surfaces in sandwich panel by 0.5

mm results in the same curve as the lowest of the three in Figure 7(a).

In stiffened panel, the load at which the yielding occurs reduces at slightly higher rate than the buckling load. Somewhat higher reduction is present in the most corroded case, but that is because of local buckling which occurs during panel global post-buckling, i.e. the failure mode changes and yielding occurs sooner. All other cases exhibit global deformation shape until the onset of plasticity.

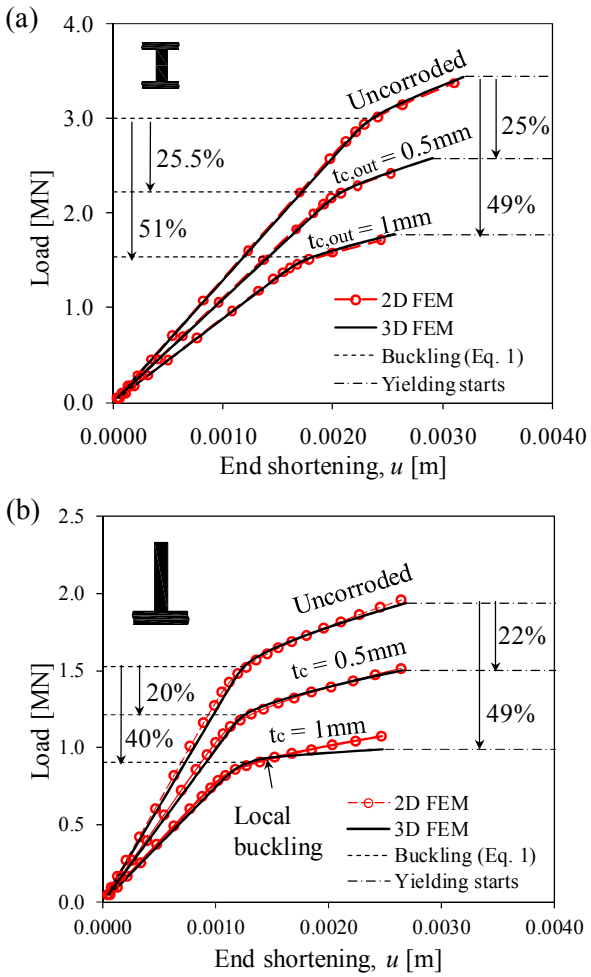

Figure 7. Influence of general corrosion on load-shortening behavior: (a) sandwich panel; (b) stiffened panel.

5. DISCUSSION AND CONCLUSION

The study focused on the influence of plate thickness reduction due to general corrosion on the buckling load and onset of plasticity in laser-welded web-core sandwich panel and stiffened panel. The two panels were selected such that their in-plane and bending stiffness in loading direction are the same. The corrosion scenario in sandwich panel is based on experimental observations. Sandwich panel is affected by general corrosion from (a) outside and (b) both inside and outside the structure. In stiffened panel, all surfaces are affected by the same extent.

In both structures, the degradation of the stiffness and the buckling load is found to depend linearly on the reduction of the thickness, following the linear reduction of stiffnesses. The reduction of buckling load is found greater in sandwich panel than in stiffened panel. For a decrease in the thickness of 0.5 mm, the reduction of the buckling load is 20% in the stiffened panel, 25.5% in the sandwich panel with outer corrosion and 51% in the sandwich panel with inner and outer corrosion. The reason for this difference was found in transverse shear stiffness opposite to web-plate direction D_{Qy} in sandwich panel which decreases the most of all stiffness coefficients.

The load at the onset of plasticity is reduced at the same rate as the buckling load, which means that the safety margin between the design point of the structure and the onset of material failure remains unaffected. The stress at the yield point are presented in Jelovica *et al.* (2014). The importance of secondary bending for estimation of yielding was presented. This feature was neglected in earlier studies tackling the material failure of web-core sndwich panels.

The agreement between 2D and 3D model results was excellent, except in the case of local buckling which is known to be beyond the capability of ESL with linear stiffness coefficients (see Reddy 1989; Jelovica and Romanoff 2013a). Nonetheless, the agreement between the two methods in the global buckling and post-buckling response validates the accuracy of stiffness coefficients of the corroded panels.

Buckling load reduction rates in sandwich panel suggest that the current guidelines for corrosion protection of these structures should be updated. Protection against corrosion should be performed with special care in these high-performing structures if their benefits are to be utilized in practice.

APPENDIX A - STIFFNESS COEFFICIENTS OF WEB-CORE SANDWICH PANEL

A symmetric web-core sandwich panel is a special type of orthotropic plate where the stiffness coefficients A_{13}, A_{23}, D_{13}, D_{23}, and B_{ij} are equal to zero. The extension stiffnesses for the orthotropic plate at hand can be expressed as

$$\begin{aligned} A_{11} &= 2E't_{\mathrm{f}} + \frac{Eh_{\mathrm{c}}}{s}t_{\mathrm{w}}; \\ A_{12} &= 2\nu E't_{\mathrm{f}}; \\ A_{22} &= 2E't_{\mathrm{f}}; \\ A_{33} &= 2Gt_{\mathrm{f}}; \end{aligned} \tag{2}$$

where $E' = E/\left(1-\nu^2\right)$. It can be seen that the extension stiffnesses depend linearly on the thicknesses of the face plate and web plate.

The bending stiffnesses are given by

$$D_{11} = \frac{h_c^3}{12}\left[2E'\left\{3\cdot\frac{t_f}{h_c}+6\cdot\left(\frac{t_f}{h_c}\right)^2+4\cdot\left(\frac{t_f}{h_c}\right)^3\right\}+E\frac{t_w}{s}\right],$$
$$D_{12} = \frac{h_c^3}{12}\left[2\nu E'\left\{3\cdot\frac{t_f}{h_c}+6\cdot\left(\frac{t_f}{h_c}\right)^2+4\cdot\left(\frac{t_f}{h_c}\right)^3\right\}\right], \quad (3)$$
$$D_{22} = \frac{h_c^3}{12}\left[2E'\left\{3\cdot\frac{t_f}{h_c}+6\cdot\left(\frac{t_f}{h_c}\right)^2+4\cdot\left(\frac{t_f}{h_c}\right)^3\right\}\right],$$
$$D_{33} = \frac{h_c^3}{12}\left[2G\left\{3\cdot\frac{t_f}{h_c}+6\cdot\left(\frac{t_f}{h_c}\right)^2+4\cdot\left(\frac{t_f}{h_c}\right)^3\right\}\right].$$

Since, typically, $t_f << h_c$, the higher-order (square and cubic) terms of the ratio (t_f / h_c) are negligible and thus have an insignificant influence on the bending stiffness coefficients, which then depend linearly on the thicknesses of the face and web plates for a constant core height h_c.
The transverse shear stiffness in the web plate direction for a symmetric plate is equal to

$$D_{Qx} = k_{11}^2\left(2G_f t_f + \frac{t_w}{s}Gh_c\right), \quad (4)$$

where

$$k_{11} = \sqrt{\frac{1}{A\left(\sum_i \int\left(\frac{\tau_i}{Q_{Qx}s}\right)^2 t_i \mathrm{d}s_i\right)}}, \quad i = \mathrm{t,c,b}. \quad (5)$$

The transverse shear stiffness in the opposite direction to the web plate direction is (for a symmetric plate)

$$D_{Qy} = \frac{12D_w}{s^2\left(k_Q\left(\frac{D_w}{D_f}+6\frac{d}{s}\right)+12\frac{D_w}{k_\theta\cdot s}-2\frac{d}{s}\right)} \quad (6)$$

where

$$k_Q = \frac{1+6\frac{D_f}{D_w}\frac{d}{s}}{2+12\frac{D_f}{D_w}\frac{d}{s}}, \quad (7)$$

The T-joint rotational stiffness is defined as the ratio of the moment M to the rotation angle θ_c at the weld (see Figure 1):

$$k_\theta = \frac{M}{\theta_c}. \quad (8)$$

APPENDIX B - STIFFNESS COEFFICIENTS OF STIFFENED PANEL

The in-plane, coupling, and bending stiffness matrices are calculated similarly as in sandwich panel, however, the integration over the height of the sandwich panel is replaced by the height of the stiffener and the plate thickness of the stiffened panel (Aavi 2012).
The elasticity matrix of the plate is

$$[E]_i = \frac{1}{1-\nu_i^2}\begin{bmatrix} E_i & \nu_i E_i & 0 \\ \nu_i E_i & E_i & 0 \\ 0 & 0 & G_i\left(1-\nu_i^2\right)\end{bmatrix}, \quad i = \mathrm{t,b}, \quad (9)$$

while the stiffener has the elasticity matrix:

$$[E]_c = \frac{E_w t_w}{s}\begin{bmatrix}1&0&0\\0&0&0\\0&0&0\end{bmatrix}. \quad (10)$$

The shear stiffness in transverse direction is:

$$D_{Qy} = k_{yz}\left(G\cdot t_p\right), \quad (11)$$

where shear correction factor k_{yz} is 5/6 and t_p is the plate thickness.
The shear stiffness in longitudinal direction is (Aavi 2012):

$$D_{Qx} = k_{xz}\left(G_p t_p + G_w h_w\right), \quad (12)$$

where G_p is the shear stiffness of the plate and G_w is shear stiffness of the stiffener:

$$G_w = G_p\frac{t_w}{s}. \quad (13)$$

Shear correction factor in longitudinal direction k_{xz} is:

$$k_{xz} = \frac{(\tau_{xz})_{avg}}{(\tau_{xz})_{max}}, \quad (14)$$

where average shear stress is approximated with:

$$(\tau_{xz})_{avg} \approx \frac{Q_z}{A_w + t_w t_p}, \quad (15)$$

and the maximum shear stress is calculated using:

$$(\tau_{xz})_{max} \approx \frac{Q_z\left[A_p\left(2z_{na}-t_p\right)+t_w\left(z_{na}-t_p\right)^2\right]}{2I_z t_w}. \quad (16)$$

A_w is the area of the flat bar and A_p is the area of the plate between two stiffeners. t_w is the thickness of the flat bar. z_{na} is the distance from the tip of the stiffener to the neutral axis and I_z is the second moment of area of stiffener and associated plate.

APPENDIX C – INFLUENCE OF MESH SIZE ON LOAD-SHORTENING CURVE AND ONSET OF PLASTICITY

The influence of mesh size on the results is studied in the case of stiffened panel with thinnest plates, i.e. the highest rate of corrosion. This is the case that is most prone to local

buckling and rapid stress development leading to yielding. The selected meshes are presented in Table C.1 and the resulting load-shortening curves are presented in Figure C.1. The curves are presented until the 355 MPa is reached at any point in the panel. Models with less than 4 elements between stiffeners omit the local buckling that occurs during global post-buckling. However, the models with coarse mesh predict the global buckling load with reasonable accuracy. Several elements are required per stiffener height since the location of yielding is the stiffener tip. Figure C.2 presents the state of deformation and stress when the yielding starts, obtained with the finest mesh used here. Increase in the number of elements leads, as expected, to improved accuracy in terms of load-shortening behavior and prediction of yield point. Mesh no.7 is selected for the remaining study since the difference in load-shortening curve and prediction of yielding is very small in comparison to the finest mesh.

Table C.1 Number of elements in the mesh and resulting buckling load.

Mesh no.	No. elements			Buckling load (MN)	Δ Buckling load
	Between stiffeners	Per stiff. height	Total in panel		
1	1	1	300	0.9317	+3.79%
2	1	3	540	0.9124	+1.64%
3	2	3	1 370	0.9138	+1.79%
4	4	3	3 890	0.9024	+0.52%
5	6	3	7 560	0.8997	+0.22%
6	8	3	12 380	0.8993	+0.18%
7	8	6	15 550	0.8984	+0.08%
8	16	8	53 760	0.8977	REF.

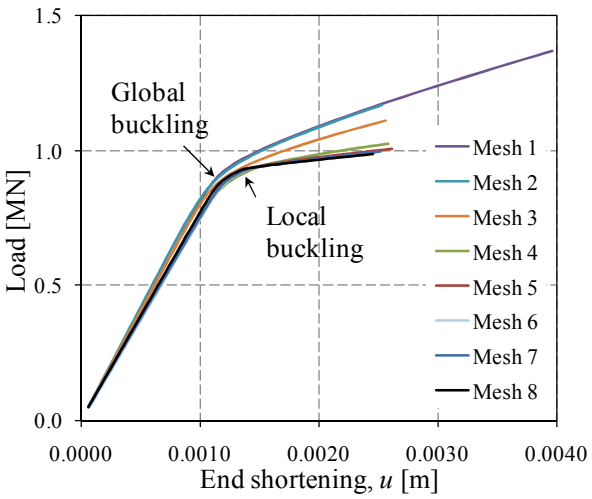

Figure C.1. Influence of mesh size in 3D model on load-shortening curve of stiffened panel.

The influence of mesh size of 2D model on the results is studied in the case of sandwich panel with thinnest plates, i.e. the highest rate of corrosion. The load-shortening curves are presented in Figure C.3. As can be seen, mesh size consisting of 25 elements in *x*- and 25 elements in *y*-direction gives good correspondence to the results of models with finer meshes. Nonetheless, the remaining study is conducted with the finest mesh since it gives the most accurate panel response and the calculation is relatively inexpensive.

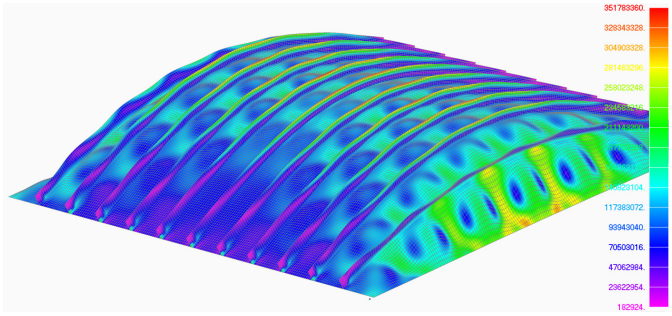

Figure C.2. Shape of the stiffened panel at the onset of plasticity with the finest mesh used (magnification factor 7.0).

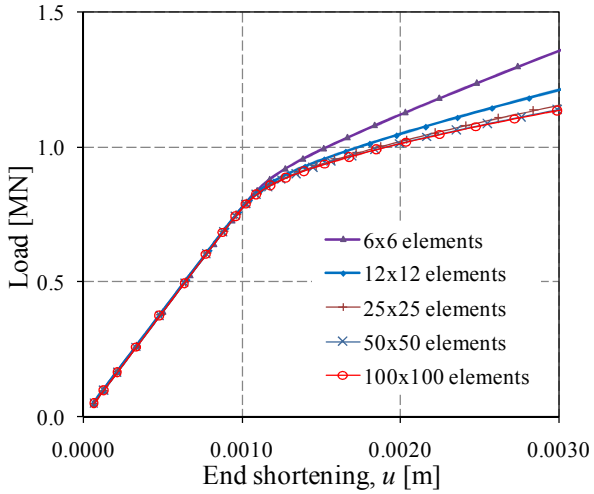

Figure C.3. Influence of mesh size in 2D model on load-shortening curve of sandwich panel.

ACKNOWLEDGMENTS

The authors gratefully acknowledge the financial support of the Sustainable Breakthrough Innovations project, funded by the Finnish Metals and Engineering Competence Cluster (FIMECC) and Finland Distinguished Professor (FiDiPro) - project "Non-linear Response of Large, Complex Thin-Walled Structures" funded by the Finnish Funding Agency for Innovation (Tekes), Deltamarin, Napa Ltd, Koneteknologiakeskus Turku, Ruukki and STX Finland. Appreciation is also due to CSC – IT Centre for Science Ltd. for providing ABAQUS software license.

REFERENCES

Aavi, E., 2012, Equivalent shell element for ship structural design. M.Sc. thesis, Aalto University.

Aromaa, J., Jelovica, J. and Forsen, O., 2012, Corrosion of laser welded sandwich steel panels in seawater. Proc. EUROCORR, Istanbul, Turkey, 9-13.9.2012; p. 1-11.

Byklum, E. and Amdahl, J., 2002, A simplified method for elastic large deflection analysis of plates and stiffened panels due to local buckling, Thin-Walled Structures 40: 925-953.

Byklum, E., Steen, E. and Amdahl, J., 2004, A semi-analytical model for global buckling and postbuckling analysis of stiffened panels, Thin-Walled Structures 42: 701-717.

Det Norske Veritas, 2003, Seawater exposure of laser-welded sandwich beams for evaluation of corrosion properties. Technical report No. 2003-1553.

Det Norske Veritas, 2004, Projected guidelines for metal-composite laser-welded sandwich panels.

Guedes Soares, C. and Gordo, J.M., 1997, Design methods for stiffened plates under predominantly uniaxial compression, Marine Structures 10: 465-497.

Gordo, J.M. and Guedes Soares, C., 2011, Compressive tests on stiffened panels of intermediate slenderness, Thin-Walled Structures 49: 782-794.

ISSC, 2009, Ultimate Strength Committee. S. Korea.

Jelovica, J., Romanoff, J., Ehlers, S. and Varsta, P., 2012, Influence of weld stiffness on buckling strength of laser-welded web-core sandwich plates, Journal of Constructional Steel Research, 77, p. 12-18.

Jelovica, J., Romanoff, J., Ehlers, S. and Aromaa, J., 2013, Ultimate strength of corroded web-core sandwich beams. Marine Structures, 31, p.1-14.

Jelovica, J. and Romanoff, J., 2013a, Load-carrying behavior of web-core sandwich plates in compression. Thin-Walled Structures, 73, p. 264-272.

Jelovica, J. and Romanoff, J., 2013b, Comparison of load-carrying behavior between web-core sandwich, stiffened and isotropic plate. In: Guedes Soares C, Romanoff J, editors. Analysis and design of marine structures. Londn: Taylor & Francis; 2013. p. 397-404.

Jelovica, J., Romanoff, J., Remes, H., 2014, Influence of general corrosion on buckling strength of laser-welded web-core sandwich plates. Submitted to Journal of Constructional Steel Research.

Kolsters, H., 2004, Structural Design of Laser-Welded Sandwich Panels for Marine Applications, Doctoral Dissertation, Royal Institute of Technology, Department of Aeronautical and Vehicle Engineering, Stockholm. Paper D: Buckling of laser-welded sandwich panels: Part 3: Ultimate strength and experiments.

Kozak, J., 2006, Problems of strength modeling of steel sandwich panels under in-plate loads, Polish Maritime Research 1: 9-12.

Masaoka, K. and Mansour, A., 2008, Compressive strength of stiffened plates with imperfections: simple design equations, Journal of Ship Research 52:3 227-237.

Melchers, R.E., Ahammed, M., Jeffrey, R. and Simundic, G., 2010, Statistical characterization of surfaces of corroded plates. Marine Structures; 23:274-87.

Nordstrand, T., 2004, On buckling loads for edge-loaded orthotropic plates including transverse shear, Composite structures 65: 1-6.

Paik, J.K., 2007, Empirical formulations for predicting the ultimate compressive strength of welded aluminium stiffened panels, Thin-Walled Structures 45: 171–184.

Paik, J.K. and Thayamballi, A.K., 2003, Ultimate limit state design of steel-plated structures. Chichester: John Wiley & Sons.

Reddy J.N., 1989, On the generalization of the displacement-based laminate theories. Appl Mech Rev, Vol. 42, No.11, part 2.

Reddy, J.N., 2000, Mechanics of laminated composite plates and shells – Theory and analysis, second ed. Boca Raton: CRC Press.

Romanoff, J., Remes, H., Socha, G., Jutila, M. and Varsta, P., 2007, The stiffness of laser stake welded T-joints in web-core sandwich structures, Thin-Walled Structures 45: 453–462.

Romanoff, J. and Varsta, P., 2007, Bending response of web-core sandwich plates, Composite Structures 81: 292-302.

Taczala, M. and Banasiak, W., 2004, Buckling of I-core sandwich panels. Journal of Theoretical and Applied Mechanics 42(2): 335-348.